Journal of Magnetic Resonance 206 (2010) 32–40

Contents lists available at ScienceDirect

Journal of Magnetic Resonance

journal homepage: www.elsevier.com/locate/jmr

The application of frequency swept pulses for the acquisition of nuclear quadrupole resonance spectra

Aaron J. Rossini, Hiyam Hamaed, Robert W. Schurko *

Department of Chemistry and Biochemistry, University of Windsor, Windsor, Ontario, Canada N9B 3P4

ARTICLE INFO

Article history:
Received 26 March 2010
Revised 20 May 2010
Available online 1 June 2010

Keywords:
Nuclear quadrupole resonance
NQR
Frequency swept pulses
Probe tuning
Wideline spectroscopy

ABSTRACT

The acquisition of nuclear quadrupole resonance (NQR) spectra with wideband uniform rate and smooth truncation (WURST) pulses is investigated. ^{75}As and ^{35}Cl NQR spectra acquired with the WURST echo sequence are compared to those acquired with standard Hahn-echo sequences and echo sequences which employ composite refocusing pulses. The utility of WURST pulses for locating NQR resonances of unknown frequency is investigated by monitoring the integrated intensity and signal to noise of ^{35}Cl and ^{75}As NQR spectra acquired with transmitter offsets of several hundreds kilohertz from the resonance frequencies. The WURST echo sequence is demonstrated to possess superior excitation bandwidths in comparison to the pulse sequences which employ conventional monochromatic rectangular pulses. The superior excitation bandwidths of the WURST pulses allows for differences in the characteristic impedance of the receiving and excitation circuits of the spectrometer to be detected. Impedance mismatches have previously been reported by Marion and Desvaux [D.J.Y. Marion, H. Desvaux, J. Magn. Reson. (2008) 193(1) 153–157] and Muller et al. [M. Nausner, J. Schlagnitweit, V. Smrecki, X. Yang, A. Jerschow, N. Muller, J. Magn. Reson. (2009) 198(1) 73–79]. In this regard, WURST pulse sequences may afford an efficient new method for experimentally detecting impedance mismatches between receiving and excitation circuits, allowing for the optimization of solids and solution NMR and NQR spectrometer systems. The use of the Carr–Purcell Meiboom–Gill (CPMG) pulse sequence for signal enhancement of NQR spectra acquired with WURST pulses and conventional pulses is also investigated. Finally, the utility of WURST pulses for the acquisition of wideline NQR spectra is demonstrated by acquiring part of the $^{63/65}$Cu NQR spectrum of CuCN.

1. Introduction

Nuclear quadrupole resonance (NQR) is often referred to as 'zero-field NMR' because it involves inducing and observing nuclear spin state transitions in the absence of large static magnetic fields [1–4]. The NQR phenomenon may be observed for quadrupolar nuclei ($I \geqslant 1$) in environments which possess non-zero electric field gradients (EFGs). EFGs arise from non-spherically symmetric charge distributions (e.g., from surrounding atoms and bonds) about a nucleus and are described by second-rank tensors which are symmetric and traceless [3,4]. Diagonalization of the EFG tensor yields three principal components (V_{jj}) which are ordered such that $|V_{11}| \leqslant |V_{22}| \leqslant |V_{33}|$. In turn, the diagonalized EFG tensor may be described by two parameters, the quadrupolar coupling constant ($C_Q = eV_{33}Q/h$) and the electric field gradient asymmetry parameter [$\eta_Q = (V_{11} - V_{22})/V_{33}$]. In a pure NQR experiment, the quadrupolar resonance frequencies (ν_Q) are determined by C_Q and η_Q. For example, there is only one quadrupole resonance frequency for an $I = 3/2$ nucleus which is given by the expression:

$$\nu_Q = \frac{C_Q}{2}\sqrt{1 + \frac{(\eta_Q)^2}{3}}$$

For higher spin nuclei, there are several NQR transitions with distinct values of ν_Q which can be related to C_Q and η_Q via different sets of expressions [5].

The C_Q and η_Q values are dependent upon the spherical and axial symmetry, respectively, of the ground state electron distribution about the quadrupolar nucleus; therefore, knowledge of these parameters can lend insight into the structure and symmetry of the local nuclear environment. For these reasons, NQR spectroscopy has found applications in a wide range of areas such as inorganic chemistry, materials science and pharmaceuticals [6–15]. There is also much interest in the use of NQR for the detection of explosives and illicit narcotics (^{14}N NQR) [16–22]. NQR is particularly useful when values of C_Q are extremely large; in such cases, NMR spectra of quadrupolar nuclei are broadened such that detection of an NMR signal can become untenable.

* Corresponding author. Fax: +1 519 973 7098.
E-mail address: rschurko@uwindsor.ca (R.W. Schurko).

1090-7807/$ - see front matter © 2010 Elsevier Inc. All rights reserved.
doi:10.1016/j.jmr.2010.05.018

In the past, frequency-swept continuous wave irradiation was utilized for acquiring NQR spectra [1–4]. However, pulsed Fourier transform techniques, such as the standard Hahn-echo sequence [23] and quadrupolar echo sequences [24–26] (Fig. 1a), are now the preferred methods for acquiring NQR spectra. Pulse sequences such as the Carr–Purcell Meiboom–Gill (CPMG) sequence [27–29] (Fig. 1b) have also been employed for signal enhancement [30,31]. These sequences have enabled the acquisition of NQR spectra of nuclei such as ^{14}N, which typically possesses low resonance frequencies and inherently low signal to noise (S/N) [21,22,32,33]. It should also be noted that CPMG-type sequences have found applications for the signal enhancement of solid-state NMR spectra [34–38].

While these techniques are successful at increasing the S/N of NQR spectra, there are several commonly encountered problems in NQR spectroscopy. The C_Q and η_Q values are related to the symmetry of the atoms surrounding a nucleus and are characteristic of the particular system under investigation. Therefore, for a given quadrupolar nucleus, resonance frequencies of near 0 MHz to 1000's of MHz are possible. The NQR experiment can be very onerous due to this large range of resonance frequencies, and most often, the experimentalist must spend a great deal of time searching for the NQR resonance(s). If the experimentalist has some prior knowledge of the approximate values of the quadrupolar parameters, the frequency search range may be reduced, and the experimental time decreased. Such information is available from a variety of sources, including previous NQR experiments on analogous systems and from theoretically calculated quadrupolar parameters (i.e., from first principles calculations). However, for many systems, such information is either unavailable or unreliable (i.e., no previous NQR data, absent/inaccurate molecular-level structures, unreliable *ab initio* calculations, etc.).

Another commonly encountered problem in NQR spectroscopy is the acquisition of spectra which are severely broadened due to a distribution of resonance frequencies, which most often arise in systems that are disordered at the atomic or molecular level. For example, Taylor et al. have extensively studied arsenic-containing glasses with ^{75}As NQR and have found that the resonances of some samples span several MHz in breadth, as opposed to resonances in ordered solids which are typically several kHz in breadth [39–43]. The limited excitation bandwidths associated with standard, high-power, rectangular pulses utilized in the Hahn-echo sequence make it necessary to increment the transmitter frequency in order to collect such broad NQR spectra [44]. Incrementing of the transmitter frequency requires re-tuning and/or re-configuration of the probe, which can be extremely time consuming. Automated NQR systems capable of scanning a wide range of frequencies have been developed to address this problem [45–49], though they are not widely available. Both manual and automated experiments benefit from broadband excitation pulses, which serve to reduce the number of frequency increments, and may aid in mapping out broad distributions of quadrupolar frequencies. In this light, several authors have discussed the development of echo sequences constructed from composite pulses which are capable of exciting broad frequency ranges [50–54]. For example, the composite echo sequence of Odin et al. is shown in Fig. 1c [54].

Recently, there has been much interest in broadband excitation pulse sequences in solid-state NMR spectroscopy; in particular, the application of *frequency swept* pulses seems to hold significant promise. Bodenhausen et al. first demonstrated the application of echo sequences employing frequency swept pulses for the acquisition of solution ^{1}H NMR spectra [55]. Similar pulses have been employed for the excitation and signal enhancement of solid-state NMR spectra of quadrupolar nuclei [56–58] and for broadband decoupling and inversion in solution NMR experiments [59–62]. Recently, Bhattacharya and Frydman have demonstrated the application of frequency swept (wideband uniform rate smooth truncated, WURST) [61] pulses for the uniform excitation of wideline solid-state NMR spectra of quadrupolar nuclei [63]. The WURST pulse is applied at a fixed transmitter frequency, with the frequency sweep achieved via simultaneous modulation of the pulse amplitude and phase. WURST pulses differ from conventional rectangular pulses not only in their amplitude and phase modulation over the duration of the pulse, but also because of their generally lower power requirements and longer lengths (typically ca. 50 μs to several ms). Our research group has recently introduced the WURST–QCPMG pulse sequence (Fig. 1d) [64]. We have demonstrated that this sequence is useful for acquiring high quality ul-

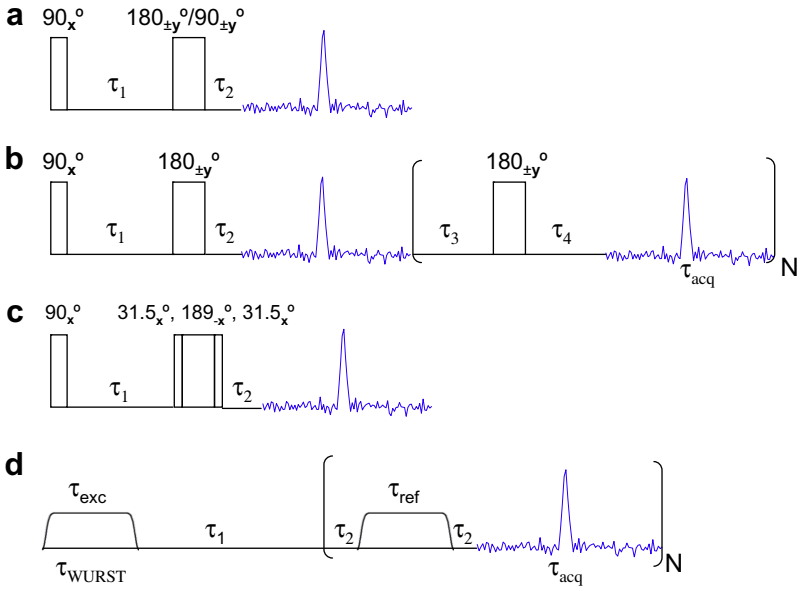

Fig. 1. Schematic representations of the pulse sequences employed for the acquisition of NQR spectra. (a) Hahn-echo with 90° excitation pulse and 180° or 90° refocusing pulse. (b) QCPMG sequence with 90° excitation pulse and a train of 180° refocusing pulses (Ref. [35]). (c) The composite echo sequence of Odin (Ref. [54]). (d) WURST–QCPMG sequence with excitation and refocusing pulses with 90° pulses of equal length and sweep rate ($\tau_{exc} = \tau_{ref}$). Note that for WURST echo spectra the WURST–QCPMG sequence (Ref. [64]) was employed with only a single refocusing pulse and the first echo was acquired ($N = 1$).

tra-wideline NMR spectra of quadrupolar nuclei; this is due in part to the large excitation bandwidths offered by the WURST pulses, and in part to the increased S/N ratios afforded by the CPMG protocol [65].

Theoretical and experimental investigations have suggested that shaped pulses suitable for NMR experiments can be readily applied to NQR experiments [66]. For instance, frequency modulated (FM) pulses have previously been applied in NQR experiments by Schurrer and Pérez [67]; however, these FM pulses possess a non-uniform "zipper"-like excitation profile limited to distinct offset frequencies. Spectral ranges greater than 500 kHz can routinely be uniformly excited with WURST pulses [64,65,68], with excitation breadth limited by a combination of the resonance frequency and probe bandwidth, suggesting that WURST echo and WURST–QCPMG sequences may find use in NQR experiments for a variety of quadrupolar nuclei.

Herein, we investigate the use of WURST echo and WURST–QCPMG sequences for the acquisition of NQR spectra. The superior excitation bandwidths of WURST pulse sequences may be helpful in locating NQR resonances during the initial stages of NQR experimentation on samples with unknown resonance frequencies. In order to mimic the search for an NQR signal of unknown frequency, spectra have been acquired with various transmitter offsets (of several hundreds of kHz) from the resonance frequencies. The signals of the NQR spectra obtained with 90°–90° echo, 90°–180° echo, Odin's composite echo sequence [54], and WURST echo pulse sequences are monitored as a function of transmitter offset frequency. The use of the CPMG protocol for signal enhancement of NQR spectra acquired with WURST pulses is investigated. The utility of the WURST pulses for the acquisition of wideline NQR spectra is also demonstrated. To this end, we have acquired a portion of the wideline $^{63/65}$Cu NQR spectrum of copper(I) cyanide (CuCN), which is a disordered solid possessing a wide distribution of $^{63/65}$Cu nuclear quadrupole resonances [69].

2. Experimental

All samples were purchased from Sigma–Aldrich Inc., and packed into shortened 5 mm glass NMR tubes. All experiments were performed on a Varian Chemagnetics triple resonance T3 MAS NMR probe with a 5 mm coil interfaced with a Varian InfinityPlus console running Spinsight software. Radiofrequency field strengths and pulse lengths were calibrated with on resonance Bloch decay experiments on the respective powdered samples. Note that we refer to the pulses which give maximum signal as "90° pulses"; however, since all experiments are performed on powdered samples these actually correspond to pulse angles of ca. 57.3° (1 radian) [54]. All "180°" pulses were double the length of "90°" pulses. For all echo experiments, the interpulse delays, τ_1 and τ_2, were set such that the full echo was acquired. Hahn-echo and QCPMG sequences employed sixteen-step phase cycles, while the composite echo sequence employed an eight-step phase cycle. The WURST–QCPMG sequence with N set equal to one was used for all WURST echo experiments (Fig. 1d) and an eight-step phase cycle was employed [63–65]. The required rf field strength (in kHz) for the WURST pulse can be approximated by, $\nu_{WURST} = A \cdot R^{1/2}(I + ½)^{-1}$, where R is the sweep rate which is equal to two times the WURST offset in kHz (e.g., a WURST offset of ±1000 kHz corresponds to a sweep range of 2 MHz) divided by the pulse length (in ms) [64]. A is a factor which ranges between 0.5 and 0.1 and is inversely proportional to the γ of the nucleus [64]. For all WURST experiments, the rf field strength of the pulse (ν_{WURST}) was experimentally optimized, starting from the theoretical value. The value of ν_{WURST} which gave maximum S/N was utilized. In all cases, WURST-80 pulse shapes were used with pulse lengths of 50 μs [61]. The WURST pulses were constructed from 900 individual pulse elements (ca. 55.6 ns in length) whose phases and amplitudes were varied to attain the desired waveform. The minimum pulse element length of the InfinityPlus waveform tool is 50 ns. The value of τ_1 for WURST experiments was set according to the formula $\tau_1 = 0.5 \cdot (\tau_{WURST} + \tau_{acq})$, where τ_{WURST} and τ_{acq} are the WURST pulse length and acquisition time of each echo, respectively. Spectral widths of 2 MHz, 1 MHz and 2.5 MHz were employed for ^{35}Cl, $^{63/65}$Cu, and ^{75}As NQR, respectively. A spectral width of 200 kHz was employed for the point-by-point $^{63/65}$Cu NQR spectrum. Recycle delays of 0.2 s, 0.4 s and 0.08 s were employed for ^{35}Cl, ^{75}As and $^{63/65}$Cu NQR experiments, respectively. Recycle delays were experimentally optimized on each sample to ensure complete longitudinal relaxation of the magnetization was obtained. All other relevant experimental parameters are listed in the Supporting information (Tables S1–S3). *CAUTION*: due to the lengths of the WURST pulses and the short recycle delays typical of NQR experiments, the duty cycle of the probe should be carefully monitored. All spectra were processed by applying three zero fills followed by Fourier transformation. For all echo spectra the full echo was acquired and Fourier transformed and the spectrum was then magnitude calculated. The S/N and integrated intensity (II) were measured with the default algorithms in the Spinsight software package. The S/N corresponds to the ratio of the peak intensity of the resonance divided by the average absolute intensity of the baseline regions. The baseline regions on either side of the NQR resonance were employed for S/N measurements. WURST–QCPMG pulse sequences for Varian (InfinityPlus–Spinsight) and Bruker (Avance–TopSpin) spectrometers are available from the authors upon request.

3. Results and discussion

^{35}Cl, $^{63/65}$Cu and ^{75}As were chosen for this work due to their high natural abundances and relatively high quadrupolar frequencies (between 34 and 116 MHz) in a variety of structural motifs. The relevant nuclear properties are listed in Table 1 [70]. All of the samples discussed herein have previously been characterized by NQR spectroscopy.

3.1. ^{75}As NQR

^{75}As NQR spectra of As_2O_3 (arsenolite phase) were previously acquired by Taylor over a range of temperatures [71]. We observed a resonance at 116.234 MHz at 294 K which is close to the frequency of 116.222 MHz (300 K) reported by Taylor. In order to mimic the initial stages of NQR experiments on a sample with unknown resonance frequencies (i.e., searching a large frequency range for a single quadrupolar resonance frequency), ^{75}As NQR spectra have been acquired at variable transmitter offset frequencies. The transmitter frequency was incremented in steps of 100 kHz for frequencies close to the NQR frequency, while a larger increment of 200 kHz was employed for offsets of 600 kHz and above. At each transmitter frequency the probe was tuned and ^{75}As NQR spectra were then acquired with the four different pulse sequences (spectra are pictured in Fig. S1 for on resonance irradiation). The integrated

Table 1
Nuclear properties [70].

Isotope	Nuclear spin	Natural abundance (%)	Quadrupole moment (Q/fm^2)	Magnetogyric ratio ($\gamma/10^7$ rad s^{-1} T^{-1})
^{35}Cl	3/2	75.8	−8.2	2.624198
^{63}Cu	3/2	69.2	−22.0	7.111789
^{65}Cu	3/2	30.8	−20.4	7.604350
^{75}As	3/2	100.0	31.4	4.596163

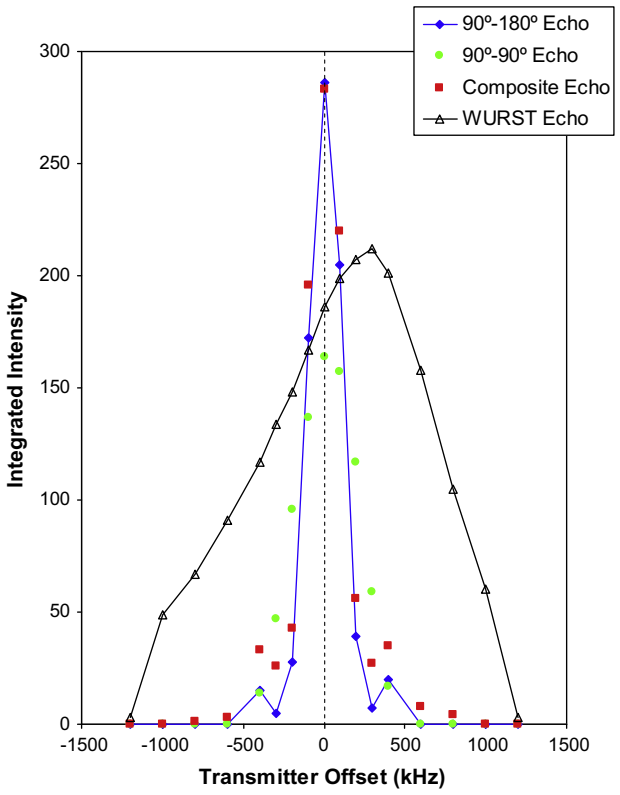

Fig. 2. Integrated intensity of the ^{75}As NQR spectra of As_2O_3 (arsenolite) as a function of transmitter offset from the resonance frequency for the 90°–180° echo, 90°–90° echo, composite echo and WURST echo pulse sequences. For each transmitter offset the probe was tuned using reflected power measurements available in Spinsight, followed by acquisition of the spectra with the four pulse sequences. For clarity the intensity points have been connected by lines for the 90°–180° echo and WURST echo spectra.

intensity (II) of the NQR spectra as a function of transmitter offset is shown in Fig. 2 (numerical values of S/N and II of the spectra are listed in Table S4).

Before the effects of transmitter offsets are reviewed it is important to discuss the factors which will influence the II and S/N of the NQR spectra acquired with the transmitter on resonance (e.g., the intensity points in Fig. 2 with 0 kHz transmitter offsets). The main factor which affects the II and S/N of all spectra acquired with echo pulse sequences is the length of time between the excitation and the refocusing pulses, during which transverse relaxation (T_2) of the magnetization occurs (i.e., the τ_1 time period in the echo sequences, Fig. 1). The τ_1 values listed in supporting information are those that were input into the pulse sequences on the spectrometer. These values are corrected within the pulse sequence programs and do not describe the total time for which the signal is allowed to dephase after the excitation pulse. For this reason, we will refer to the total dephasing time period as τ_d. Values of τ_d employed for experiments are also listed in the supporting information.

In the case of the echo sequences employing conventional pulse sequences, τ_d will be close in value to τ_1 due to the relatively short pulse widths of conventional refocusing pulses. However, the WURST echo sequence utilizes pulse widths which are much longer than conventional pulses (i.e., 50 μs). Subsequently, significantly more transverse relaxation occurs from the time a particular frequency isochromat is excited by a WURST pulse to the time it is refocused by the next WURST pulse, in comparison to conventional echo sequences. For these reasons the τ_1 values are corrected within the pulse sequence to account for lengths of the WURST pulses and for the WURST echo sequence and $\tau_d = \tau_1 + \tau_2$. The S/N and II of the 90°–180° echo sequences and WURST echo sequences with various τ_d times are listed in Table S5. The value of τ_d dramatically affects the II and S/N of the 90°–180° echo and WURST echo spectra due to the relatively short $T_2(^{75}As)$ value for As_2O_3 at room temperature. For example, NQR spectra acquired with the 90°–180° echo sequence using τ_d values of 145.7 μs and 78.35 μs, yield II values of 286 and 443, respectively. It should be noted that if τ_d is too short, it is not possible to acquire the full echo, and this truncation leads to lineshape and baseline distortions, making it difficult to obtain meaningful II and S/N measurements. For these reasons, we set τ_d for all echo experiments such that the full echo was acquired and the values of τ_d are approximately equal.

There are several key observations that can be made from Fig. 2. First, we will consider the case where the transmitter is on resonance or close to the resonance frequency (less than a 100 kHz offset). It is clear that NQR spectra acquired with the 90°–180° echo and composite echo sequences possess higher II (II > 280) and S/N (S/N > 1200) than those acquired with the WURST echo sequence (II = 186, S/N = 871). For the WURST spectra acquired on resonance we tested the effects of the rf field of the WURST pulse on the II and S/N of NQR spectra. Experiments conducted with variable WURST pulse widths (and different experimentally optimized rf field strengths) show no appreciable variation in II (Table S6). We therefore attribute the reduced II and S/N of the WURST echo to the fact that the refocusing pulse is acting as a 90° pulse since it is the same length and power as the initial pulse (e.g., the II and S/N of the WURST echo sequence are similar to the 90°–90° echo sequence).

In order to try and improve the S/N of the WURST echo spectra we have attempted to implement a 90°–180° WURST echo sequence. Bhattacharya and Frydman previously outlined several approaches for obtaining a WURST 180° (π) refocusing pulse for solid-state NMR of quadrupolar nuclei [63] The first approach is to employ a WURST π-pulse which sweeps over the range of frequencies at double the rate of the excitation pulse ($R_{ref} = 2R_{exc}$). This can be accomplished in two ways: (1) by employing a WURST π-pulse which is half the time length of the excitation pulse ($\tau_{exc} = 2\tau_{ref}$) and sweeps over the same frequency range, or, (2) by employing a WURST refocusing pulse which is identical in length to the excitation pulse ($\tau_{exc} = \tau_{ref}$), but sweeps over double the frequency range. They found that the optimal rf field for the refocusing WURST π-pulse (ν_{ref}) was ca. 4.7 times higher than that of the excitation pulse (ν_{exc}), [63] while we found experimentally optimized ν_{ref} values which were ca. 1.5–1.7 times higher than ν_{exc} (Table S7). In both cases, our "90°–180°" WURST echo spectra are similar to the corresponding 90°–90° WURST echo spectra in terms of S/N and II (Table S7). A second approach for obtaining a WURST π-pulse is to utilize a refocusing pulse of the same length ($\tau_{exc} = \tau_{ref}$) and same sweep rate ($R_{ref} = R_{exc}$); however, ν_{ref} is set to ca. 3.2 times larger than ν_{exc}. In this case, we found that maximum signal is obtained when $\nu_{exc} \approx \nu_{ref}$ (identical to a 90°–90° WURST echo spectrum), consistent with our previous results obtained from the solid-state NMR spectra of quadrupolar nuclei [64]. It is worth noting that the WURST pulses employed herein are much shorter (less than 100 μs) than those employed by Bhattacharya and Frydman (ca. 1–2 ms), and hence, the pulses may be operating in different adiabatic regimes (this may account for the differences in ratios of ν_{ref}:ν_{exc} between our experiments and Frydman's experiments). It may be possible to obtain WURST π-pulses by employing longer pulse widths, however, this would necessitate the use of much longer echo delays and result in NQR spectra with lower S/N.

At relatively large transmitter offsets (i.e., 200 kHz and greater) the WURST echo sequence affords higher II and S/N NQR spectra than those acquired with conventional echo sequences. For instance, with WURST pulses, NQR spectra with II > 48 are observed for transmitter offsets as large as 1000 kHz. Clearly, the WURST

pulses offer superior excitation bandwidths in comparison to the conventional rectangular pulses. Considering these observations, a strategy for the observation of NQR resonances of unknown frequencies emerges. The frequency range of interest can be surveyed with a WURST echo or WURST–QCPMG sequence using large transmitter offset increments. In this case, transmitter increments of ca. 2000 kHz could be reasonably employed with the WURST echo sequence in the search for an NQR resonance of unknown frequency, while the composite echo sequence would be limited to transmitter increments of ca. 800 kHz. Once the approximate frequency of the NQR resonance is identified, the transmitter could be set to the resonance frequency and a high quality spectrum could then be obtained with a conventional sequence.

Another important observation is the distinct asymmetry in the peak intensities in Fig. 2. For all of the pulse sequences, higher intensities are observed for spectra acquired with positive transmitter offsets in comparison to those acquired with negative transmitter offsets of the same magnitude. This asymmetry is particularly pronounced for the WURST echo spectra. For example, for the WURST echo spectrum acquired at an offset of +300 kHz, II = 212, while at an offset of −300 kHz, II = 134. Additionally, the WURST echo NQR spectra unexpectedly possess higher II when the transmitter is +300 kHz from resonance (II = 212), rather than when the transmitter is on resonance (II = 186).

What is the origin of this asymmetry in II and S/N for equally spaced transmitter offsets of opposite sign? Initially, we thought this asymmetry may be due to the sweep direction of WURST pulses. Given the lengths of the WURST pulses (50 μs) and the fact that the pulse is linearly swept across the specified frequency range, it is possible that transverse relaxation (T_2) of the resonance may occur if the resonance is excited near the start of the first WURST pulse waveform; however, when a pulse with opposite sweep direction was applied, spectra with an identical intensity profile were obtained (not shown). Our research group has previously observed similar asymmetries in ^{14}N WURST–QCPMG NMR spectra, which were found to result from frequency sweep induced population transfers [68]. However, this is very unlikely, given that there are only two quantized energy levels, and that this asymmetry is observed in spectra using WURST pulses with opposite sweep directions. Both of these mechanisms are unlikely, given that this asymmetry in intensities is observed for all of the other pulse sequences, although, the asymmetry is not as pronounced as for the WURST echo spectra.

Therefore, we attribute the asymmetry in Fig. 2 to a difference in the characteristic impedance values of the excitation circuit and receiver circuit of the spectrometer (which we refer to as an "impedance mismatch"). This phenomenon has recently been reported by Marion and Desvaux [72] and Muller et al. [73]. In both manuscripts, the authors describe the observation of an impedance mismatch via the acquisition of spin-noise NMR spectra. It was found the S/N of the spin-noise NMR spectra improved when the probe was detuned (as indicated by standard tuning protocols). This is because the standard tuning procedures available with most commercial spectrometers result in tuning of the probe such that it is optimized for excitation (e.g., matched and tuned to the amplifier circuit), rather than for receiving of signals [72,73]. These impedance mismatches are readily detected in spin-noise NMR spectra, because they require no excitation pulses and their S/N and phases are only dependent upon impedance matching the probe to the receiver.

In our work the probe was coarsely tuned by observing an impedance–frequency response curve (e.g., a 'wobble' curve) and fine tuned by minimizing the level of reflected power. This method optimizes the tuning of the probe for excitation only. Fig. 2 indicates that there is an approximate difference of 300 kHz between the optimal receiver and excitation tuning of the probe, which is consistent with the frequency differences of several hundred kilohertz observed by Desvaux and Muller et al. [72,73]. In order to confirm that there was an impedance mismatch, the probe was tuned in the usual manner to 116.534 MHz, which is 300 kHz *higher* than the resonance frequency. The transmitter frequency was then placed on resonance (116.234 MHz), and spectra with the five different pulse sequences were acquired. This yielded spectra with higher II and S/N, except for the spectrum acquired with 90°–90° echo sequence (Fig. 3, spectra are shown in Fig. S2). Finally, additional experiments were conducted which involved re-calibration of the pulse widths to account for the de-tuning of the probe (the 90° pulse width increases from 1.6 μs to 2.1 μs). These experiments yield S/N and II values which are between 1.3 and 1.4 times larger than those obtained when the probe is tuned to the transmitter frequency (i.e., on resonance). These gains are observed for all of the pulse sequences (compare first data set to last data set for each pulse sequence in Fig. 3).

We have also investigated the influence of the receiver gain setting on the II and S/N values when the probe is optimized for excitation (tuned on resonance) and when the probe is optimized for reception (tuned +300 kHz off resonance) and re-calibrated pulse widths are employed (Table S8). The II is observed to steadily increase with the receiver gain level, while the S/N ratio remains constant. Marion and Desvaux have observed that at higher receiver gain settings, the S/N ratio of solution ^{1}H NMR spectra is progressively lowered and balances the gains in signal (II), due to uniform digitization of the probe noise at higher receiver gain settings [72]. However, they also point out that if the pre-amplifier noise level is significant, then it is expected that tuning the probe to the receiver optimum will always lead to improved S/N ratios [72]. This suggests that in our system, the pre-amplifier is the

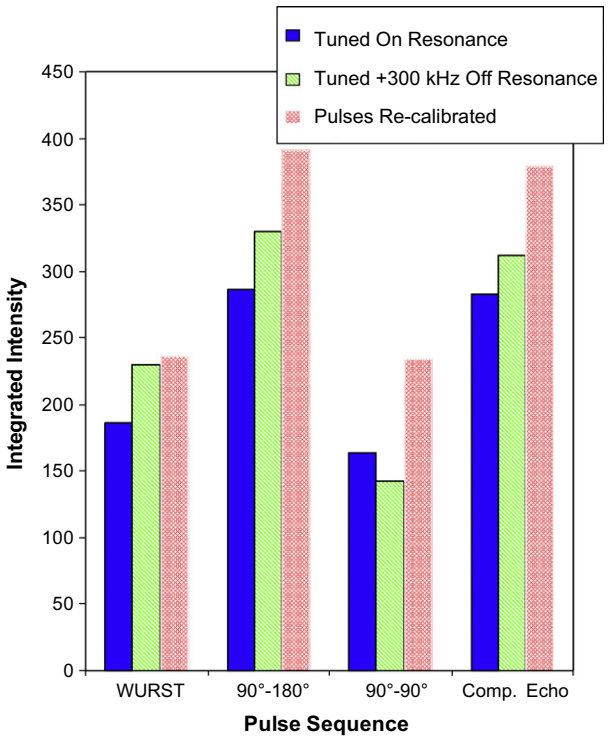

Fig. 3. Integrated intensity of the ^{75}As NQR spectra of As_2O_3 acquired when the probe has been tuned on resonance (116.234 MHz), tuned +300 kHz off resonance (116.534 MHz), and when the probe is tuned +300 kHz off resonance and the pulse widths have been re-calibrated. The transmitter was set to the resonant frequency (116.234 MHz) in all cases. Spectra were acquired with the four different pulse sequences. When the probe is tuned +300 kHz off resonance and re-calibrated pulses are employed, the II of the NQR spectra is 1.3–1.4 times larger.

predominant noise source, as we observe improved S/N ratios when the probe is tuned to the receiver optimum for a range of receiver gain settings.

The superior excitation bandwidths of the WURST pulses enable experiments which allow for the detection of impedance mismatches between reception and excitation pathways, even when the differences are on the order of several 100 kHz. WURST echo spectra could be acquired with variable offsets and the II or S/N can be plotted in a manner similar to that presented herein to detect the optimal receiver tuning. Marion and Desvaux have demonstrated that this mismatch can be eliminated by altering the impedance of the amplifier pathway by changing the lengths of transmission cables [72]. In the future, we intend to utilize the WURST echo sequence in order to better impedance match our reception and excitation pathways. This approach should be applicable to NQR, as well as solution and solids NMR experiments, and would be much faster than acquiring spin-noise NMR spectra. It would also be possible to detect impedance mismatches by monitoring the S/N of a spectrum acquired with conventional pulses while the transmitter is placed on resonance and the probe tuning frequency is varied. However, if there is a large impedance mismatch, the pulse widths of the conventional pulses will increase due to reflection of power by the probe [72]. This necessitates time consuming pulse width calibrations for each probe tuning increment. Therefore, WURST pulses should be better suited to detect impedance mismatches.

3.2. Signal enhancement with the CPMG protocol

Marino and Klainer first demonstrated in 1977 that the CPMG pulse sequence affords large S/N gains in NQR [31]. CPMG-type sequences are now frequently employed in order to enhance the signal of unreceptive NQR nuclei such as ^{14}N [18,21,22,30]. For these reasons, the S/N of ^{75}As NQR spectra acquired with the QCPMG [35] and WURST–QCPMG sequences [64]. (Fig. 1) are compared to the corresponding single echo sequences. In order to obtain "spikelet-free" spectra, the spin echoes obtained from the ^{75}As QCPMG and WURST–QCPMG FIDs were summed into a single time domain echo [74]. These single time domain echoes were then Fourier transformed to produce spectra which are similar in appearance to conventional echo spectra [74]. The QCPMG and WURST–QCPMG spectra are compared to echo spectra in Fig. S3 and II and S/N measurements are shown in Table 2. The QCPMG spectra are of higher II and S/N than the WURST–QCPMG when the number of echoes (MG loops) and echo size is the same. This is consistent with the II and S/N observed for the corresponding echo sequences.

While the T_2(^{75}As) and T_1(^{75}As) time constants are relatively short for As_2O_3 at room temperature it is possible to acquire multiple echoes for ca. 4.5 ms. It can be readily seen that the acquisition of multiple echoes yields significant improvements in II and S/N of the NQR spectra. For example the acquisition of 8 MG loops leads to ca. threefold increase in the II values for both the WURST–QCPMG and QCPMG pulse sequences, in comparison to the corresponding single echo experiments. As expected for CPMG experiments, the largest signal enhancements are obtained when a large number of tightly spaced echoes are acquired. When the echo size is 256 points and 24 echoes are acquired the II is observed to increase by factors of 12.3 and 13.4 for WURST–QCPMG and QCPMG, respectively. Acquisition of 80 echoes (with each echo consisting of 140 points) leads to gains in the II by factors of 28 and 32 for the WURST–QCPMG and QCPMG sequences, respectively (last entries, Table 2). However, it should be noted that when the echo size is small, truncation of the individual echoes results in broadening of the NQR resonances as well as baseline distortions (Fig. S3), rendering the measured II and S/N values unreliable. Clearly, the CPMG protocol can be used to enhance the signal of NQR spectra acquired with WURST pulses. The WURST–QCPMG sequence can provide significant signal enhancement and should make WURST pulses more competitive with conventional pulses, while still retaining their larger excitation bandwidths.

Table 2
Integrated intensity and signal to noise of single echo and QCPMG ^{75}As NQR spectra.

Echo size	τ_{acq} (μs)	MG Loops (N)[a]	WURST–QCPMG[b]		QCPMG[c]	
			II	S/N	II	S/N
512	204.8	1	186	871	286	2506
512	204.8	8	624	2064	904	3293
256	102.4	24	2294	4700	3834	5741
[d]140	56.0	80	5227	4117	9172	5427

[a] This is the number of refocusing pulses and echoes that were acquired. For the case of MG Loops = 1 the II and S/N from the 90°–180° echo and WURST echo spectra were used.
[b] For all WURST–QCPMG experiments τ_2 = 20 μs. τ_1 can be determined using the formula given in the Experimental section.
[c] For all QCPMG experiments τ_2 = 30 μs and τ_3 = τ_4 = 20 μs.
[d] Small echo sizes lead to truncation of the individual echoes in the time domain. This causes lineshape and baseline distortions leading to skewed II and S/N values.

3.3. ^{35}Cl NQR

A series of experiments similar to that described above has been conducted for the acquisition of ^{35}Cl NQR spectra of 4-chloropyridine. This was done in order to test the use of WURST pulses for the acquisition of spectra of a less receptive NQR nucleus and the performance of the sequence at a lower resonance frequency. The ^{35}Cl NQR spectrum of 4-chloropyridine at a temperature of 77 K was acquired by Bray et al. and a resonance at 34.789 MHz was observed [75]. We observed a resonance at 35.352 MHz at a temperature of 294 K. In Fig. 4, the II of the ^{35}Cl NQR spectra as a function

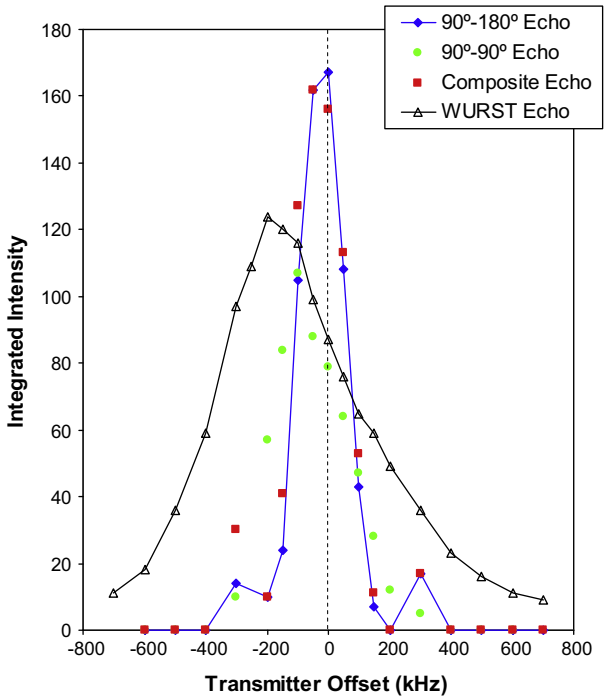

Fig. 4. Integrated intensity of the ^{35}Cl NQR spectra of 4-chloropyridine as a function of transmitter offset from the resonance frequency for the 90°–180° echo, 90°–90° echo, composite echo and WURST echo. For each transmitter offset the probe was tuned using reflected power measurements available in Spinsight. Spectra with the four pulse sequences were then acquired. For clarity the intensity points have been connected by lines for the 90°–180° echo and WURST echo spectra.

of transmitter offset is shown (II and S/N values given in Table S9) for the four different pulse sequences. Spectra acquired with the four pulse sequences and the transmitter on resonance are pictured in Fig. S4. This sample possesses a relatively long $T_2^*(^{35}Cl)$, and hence, a fairly long τ_d value (ca. 275 μs) is required to acquire the full echo.

From Fig. 4 it is once again clear that conventional echo pulse sequences provide superior S/N in comparison to the WURST sequence for spectra acquired with small transmitter frequency offsets (less than 100 kHz). At large frequency offsets (150 kHz and higher) the WURST pulses are much more efficient. ^{35}Cl NQR spectra of II and S/N of 18 and 13, respectively, may be observed with WURST pulses at transmitter offsets as large as 600 kHz. Therefore, in an NQR experiment involving the search for an unknown quadrupolar resonance of a similar frequency to this, it would be possible to use 1.2 MHz transmitter increments to locate the resonance, as opposed to ca. 600 kHz with conventional echoes, effectively reducing the total number of experiments by a factor of two.

The ^{35}Cl NQR configuration of the spectrometer components once again displays an impedance mismatch between the excitation and receiving pathways. In this case the receiving optimum is located at ca. −200 kHz from the excitation optimum as indicated in Fig. 4. The II was measured for the peaks in the ^{35}Cl NQR spectra acquired with the probe tuned on resonance (35.352 MHz) and tuned −200 kHz off resonance (35.152 MHz), with the transmitter fixed on resonance in both cases (Fig. 5). II and S/N increases of ca. 1.6 are observed when the probe is tuned to −200 kHz from the resonance frequency and the pulse widths are re-calibrated. These gains in II and S/N are once again relatively constant for a variety of receiver gain settings (Table S10). Although there is a smaller frequency difference between the receiving and the excitation optimum for the ^{35}Cl NQR probe configuration, the drop off in S/N is more severe than that observed for the ^{75}As NQR spectra. We attribute this to the decreased bandwidth of the probe for the ^{35}Cl NQR configuration (*vide infra*).

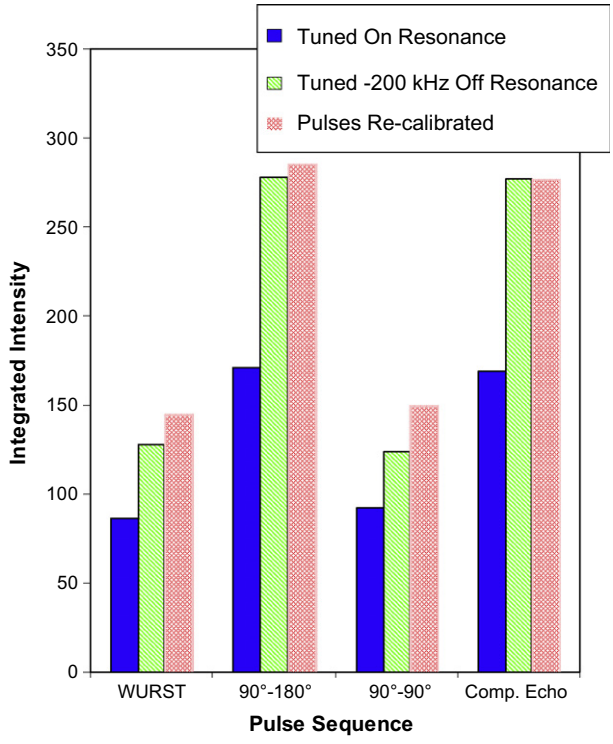

Fig. 5. Integrated intensity of the ^{35}Cl NQR spectra of 4-chloropyridine acquired when the probe has been tuned on resonance (35.352 MHz), tuned −200 kHz off resonance (35.152 MHz) and when the probe is tuned −200 kHz off resonance and the pulse widths have been re-calibrated. The transmitter was set to the resonant frequency (35.352 MHz) in all cases. Spectra were acquired with the four different pulse sequences. When the probe is tuned −200 kHz off resonance and re-calibrated pulses are employed, the II of the NQR spectra is 1.64–1.67 times larger.

3.4. Factors limiting the excitation bandwidth of WURST pulses

While the WURST pulses display impressive excitation bandwidths, it is worthwhile to consider the factors which limit them. For example, ^{35}Cl and ^{75}As NQR experiments employed WURST pulses with a sweep range of ±1000 kHz and ±1400 kHz, respectively, while resonances with offsets larger than 600 kHz and 1200 kHz, respectively, possess very low S/N. In these cases, the bandwidth and quality factor (Q-factor) of the probe are the main limitations on the apparent excitation bandwidth of the WURST pulses. The Q-factor of the probe determines the power profile of the probe, which affects both the efficiency of excitation pulses as well as the detection of signal(s).

Muller et al. have suggested that the Q-factor of the probe can be approximated by dividing the resonance frequency (ν_Q) by the FWHH measured from the inflection of the wobble curve [73]. For the ^{35}Cl NQR configuration of the probe (35.346 MHz) a FWHH value of approximately 350 kHz was observed in the wobble curve giving a Q-factor of approximately 101 (Fig. S6). For the ^{75}As NQR probe configuration (116.234 MHz) a FWHH value of approximately 600 kHz was observed in the wobble curve giving a Q-factor of approximately 194. The large probe bandwidth of the ^{75}As NQR experiments enables resonances to be detected at offsets larger than ±1000 kHz, whereas the smaller probe bandwidth in the ^{35}Cl configuration limits detection of signals to offsets of ca. ±600 kHz. For a given resonance frequency lower Q values will lead to larger probe bandwidths; however, the signal is also proportional to the Q-factor of the probe [76]. For nuclei such as ^{75}As and ^{35}Cl which are highly abundant and typically possess high resonance frequencies (and high S/N), it may be worthwhile to attempt experiments with lower Q-factor probes. This could afford larger excitation and detection bandwidths at the expense of lower S/N. Aside from limitations imposed by the probe, the required power for the WURST pulses also increases with increasing sweep width, necessitating the use of high-powers and/or longer pulses. Large sweep widths and/or long pulse lengths may lead to unacceptably high transmitter duty cycles, although sweep widths of ±1.5 MHz can be safely achieved for almost all nuclei with 50 μs WURST pulses.

3.5. Acquisition of wideline NQR spectra

Systems such as amorphous glasses [10], semiconductors [43], polymers [2] and high temperature superconductors [9,11,15] possess varying degrees of disorder at the atomic level which results in distributions in C_Q and η_Q. This in turn gives rise to distributions of NQR frequencies and correspondingly broad NQR spectra. Two methods for acquiring wideline NQR spectra are commonly employed. The traditional method involves stepping the transmitter frequency in evenly spaced increments and acquiring a spin-echo at each frequency (we will refer to this as the "point-by-point" method) [43]. The echo intensities are then plotted as a function of transmitter frequency and used to construct the NQR spectrum. The second approach is similar to the first approach in that spin-echoes are acquired at evenly spaced transmitter increments; however, each echo is Fourier transformed and then co-added in the frequency domain to form the total spectrum [44,77]. Wideline solid-state NMR spectra are frequently acquired in this manner as well [78,79]. This method is advantageous because it enables sharp spectral features to be detected while requiring fewer transmitter offsets than the point-by-point method. The superior excitation

bandwidths of the WURST pulses should make them ideal for acquiring wideline NQR spectra in a similar manner.

In order to investigate the utility of WURST pulses for the acquisition of wideline NQR spectra, we have acquired a portion of the $^{63/65}$Cu NQR spectrum of copper(I) cyanide. The $^{63/65}$Cu NQR spectrum of CuCN consists of four broad peaks (FWHH > 400 kHz) separated by several MHz with some of the peaks containing overlapping ^{65}Cu and ^{63}Cu resonances from distinct chemical environments [69]. We have acquired the approximately 1 MHz broad $^{63/65}$Cu resonance centered at 37.9 MHz (Fig. 6). The QCPMG sequence was used to acquire a point-by-point spectrum (Fig. 6a) by summing the echoes in the QCMPG echo train in the time domain [74]. The resultant echo was then magnitude calculated and the II was measured and plotted as a function of transmitter frequency. Echo intensities were measured at 15 transmitter offset frequencies, with 4000 scans per sub-spectrum (0.08 s recycle delay) and a total experimental time of 1.3 h. The asymmetric shape of the point-by-point spectrum is consistent with the previously reported spectrum [69].

The QCPMG and WURST–QCPMG spectra are shown in Fig. 6b and c, respectively. Both spectra were formed by Fourier transforming the individual sub-spectra and co-adding them in the frequency domain. Spikelet spectra and echo spectra are shown for both pulse sequences. Spikelet spectra were obtained by directly Fourier transforming the train of echoes from the CPMG spectra. Echo spectra were obtained from the QCPMG spectra in the manner described in the "Signal enhancement with the CPMG protocol" section. A transmitter increment of 120 kHz was employed for the QCPMG sequence (90° pulses of 0.7 μs); while a transmitter increment of 250 kHz was employed with the WURST–QCPMG sequence (±1000 kHz sweep ranges). This enabled the WURST–QCPMG spectrum to be acquired with only six sub-spectra while the QCPMG spectrum required 12 sub-spectra to form the total pattern. However, the lower S/N of the WURST spectra required that 6000 scans be acquired for each sub-spectrum, while only 4800 scans were required with the QCPMG sequence to obtain similar S/N ratios. It can also be seen that the spikelet and echo versions of the QCPMG and WURST–QCPMG spectra provide an excellent overall match with the shape of the point-by-point spectrum, indicating that accurate lineshapes can be obtained with either sequence [80]. However, despite the lower S/N of the WURST–QCPMG spectra the pattern could be acquired in a total time of 0.8 h, while 1.3 h of time were required for the QCPMG sequence. This also does not include the additional time required for the spectrometer operator to step the transmitter frequency and retune the probe. WURST–QCPMG is clearly the most efficient method for acquiring broad NQR spectra. It should also be noted that due to the high γ of the $^{63/65}$Cu nuclei, only ca. 100 W of input power were required for the WURST pulses, compared to ca. 750 W of input power utilized for the QCPMG spectra.

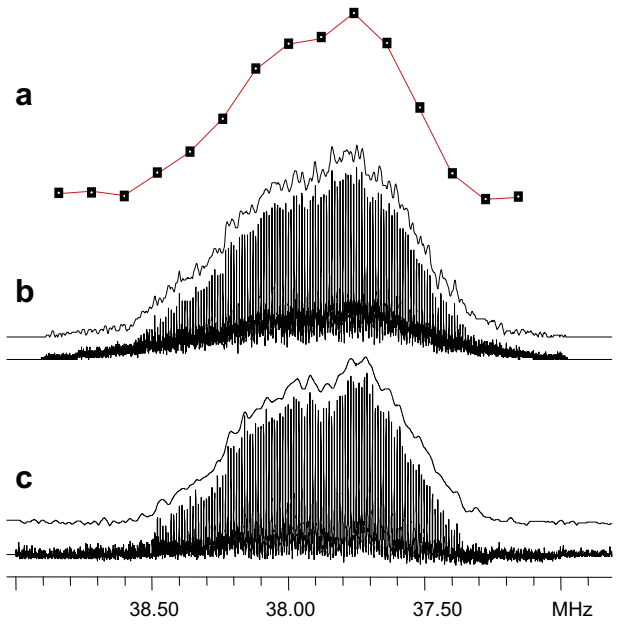

Fig. 6. Wideline $^{63/65}$Cu NQR spectrum of the broad resonance of CuCN centered around 37.9 MHz. (a) "Point-by-point" spectrum (see text for details) acquired with the QCPMG pulse sequence and low power pulses (10 μs 90° pulse). A transmitter increment of 120 kHz was employed and 15 echoes were acquired (1.3 h total acquisition time). (b) QCPMG spikelet spectrum and echo spectrum formed from time domain co-addition of the echoes. A transmitter increment of 120 kHz and high-power 90° pulses (0.7 μs) were employed. Twelve sub-spectra were required to form the total pattern (1.3 h total acquisition time). (c) WURST–QCPMG spikelet spectrum and echo spectrum formed from time domain co-addition of the echoes. A transmitter increment of 250 kHz was employed and six sub-spectra were required to form the total pattern (0.8 h total acquisition time).

4. Conclusions and future outlook

WURST echo and WURST–QCPMG experiments possess several advantages in comparison to standard pulsed experiments for the acquisition of NQR spectra. The large uniform excitation bandwidths of the WURST pulses should enable NQR signals of unknown frequency to be located in a more efficient manner than conventional pulsed NQR experiments. The broadband excitation of the WURST pulses makes them useful for samples which possess broad distributions of NQR frequencies, as evidenced by acquisition of $^{63/65}$Cu NQR spectra of CuCN. WURST pulses could also potentially be useful for examining samples containing multiple sites which possess disparate NQR frequencies that cannot be uniformly excited by conventional pulse techniques. However, WURST pulses are not ideally suited for samples which possess very short transverse relaxation times (T_2) and/or nuclei which possess inherently low signal spectra due to low resonance frequency and/or low natural abundance. Clearly, spectra acquired with WURST pulses are of lower S/N than those acquired with conventional echo sequences; therefore WURST experiments may be limited to nuclei which are highly receptive to NQR experiments. Impedance mismatches between receiving and excitation pathways within NQR and NMR spectrometer systems can also be readily detected with WURST pulse sequences. This may afford a straightforward method for optimizing the performance of a variety of NQR and NMR spectrometers. This is especially important for NMR or NQR experiments performed on unreceptive nuclei where it is desirable to maximize inherently weak signals.

While this work has been limited to $I = 3/2$ nuclei, it is anticipated that WURST pulses may be useful for higher spin nuclei (e.g., $I = 1, 2, 5/2$, etc.); however, due to scaling of the pulse widths, the higher spin nuclei possess inherently shorter 90° pulse widths with large excitation bandwidths. Pre-polarization schemes where the sample is shuttled in and out of high field magnets should also be compatible with WURST pulses. The large excitation bandwidths afforded by the WURST pulses in combination with their low power requirements may also make them attractive for portable NQR systems where small power supplies are desirable and/or for experiments conducted with large-diameter sample coils.

Acknowledgments

The Natural Sciences and Engineering Research Council (NSERC, Canada), the Canadian Foundation for Innovation and the Ontario Innovation Trust are acknowledged for financial support. AJR thanks NSERC of Canada for a doctoral scholarship. HH thanks

the Ministry of Training, Colleges and Universities for an Ontario Graduate Scholarship, and UW for a Tuition Scholarship. RWS thanks the Ontario Ministry of Research and Innovation for an Early Researcher Award, and acknowledges the Centre for Catalysis and Materials Research at the University of Windsor for additional funding. Dr. Luke A. O'Dell is acknowledged for programming WURST pulse sequences. Prof. Charles L.B. Macdonald (Windsor) is thanked for providing the sample of arsenic oxide. Prof. Stephen Loeb (Windsor) is thanked for providing the samples of copper cyanide and 4-chloropyridine. We thank Prof. Alexej Jerschow (New York University) for helpful discussions.

Appendix A. Supplementary material

Supplementary data associated with this article can be found, in the online version, at doi:10.1016/j.jmr.2010.05.018.

References

[1] R.S. Drago, Nuclear quadrupole resonance spectroscopy, in: Physical Methods in Chemistry, Saunders College Publishing, 1977. pp. 510–529.
[2] G.K. Semin, T.A. Babushkina, G.G. Yakobson, Nuclear Quadrupole Resonance in Chemistry, John Wiley and Sons, New York, 1975. p. 517.
[3] E.A.C. Lucken, Nuclear Quadrupole Coupling Constants, Academic Press, London, 1969. p. 360.
[4] T.P. Das, E.L. Hahn, Nuclear Quadrupole Resonance Spectroscopy, vol. 1, Academic Press, New York, 1958. p. 223.
[5] G.K. Semin, Russ. J. Phys. Chem. A 81 (1) (2007) 38–46.
[6] A. Rigamonti, Adv. Phys. 33 (2) (1984) 115–191.
[7] P. Jonsen, Prog, Nucl. Magn. Reson. Spectrosc. 27 (1995) 647–727.
[8] G. Le Caer, R.A. Brand, J. Phys. – Condes. Matter. 10 (47) (1998) 10715–10774.
[9] A. Rigamonti, F. Borsa, P. Carretta, Rep. Prog. Phys. 61 (10) (1998) 1367–1439.
[10] P.J. Bray, Inorg. Chim. Acta 289 (1–2) (1999) 158–173.
[11] A.W. Hunt, P.M. Singer, A.F. Cederstrom, T. Imai, Phys. Rev. B 64 (13) (2001) 134525-1–134525-25.
[12] H.D. Lutz, J. Mol. Struct. 646 (1–3) (2003) 227–236.
[13] A. Jerschow, Prog. Nucl. Magn. Reson. Spectrosc. 46 (1) (2005) 63–78.
[14] J.N. Latosinska, J. Pharm. Biomed. Anal. 38 (4) (2005) 577–587.
[15] R. Ofer, A. Keren, Phys. Rev. B 80 (22) (2009) 2245211-8.
[16] S.D. Somasundaram, A. Jakobsson, J.A.S. Smith, K. Althoefer, IEEE Trans. Geosci. Remote Sens. 45 (4) (2007) 925–933.
[17] A.N. Garroway, M.L. Buess, J.B. Miller, B.H. Suits, A.D. Hibbs, G.A. Barrall, R. Matthews, L.J. Burnett, IEEE Trans. Geosci. Remote Sens. 39 (6) (2001) 1108–1118.
[18] J.P. Yesinowski, M.L. Buess, A.N. Garroway, M. Ziegeweid, A. Pines, Anal. Chem. 67 (13) (1995) 2256–2263.
[19] R.A. Marino, R.F. Connors, J. Mol. Struct. 111 (December) (1983) 323–328.
[20] R. Blinc, J. Seliger, D. Arcon, P. Cevc, V. Zagar, Phys. Status Solidi A – Appl. Res. 180 (2) (2000) 541–545.
[21] T.N. Rudakov, P.A. Hayes, J.H. Flexman, Solid State Nucl. Magn. Reson. 33 (3) (2008) 31–35.
[22] A. Gregorovic, T. Apih, J. Magn. Reson. 198 (2) (2009) 215–221.
[23] E.L. Hahn, D.E. Maxwell, Phys. Rev. 88 (1952) 1070–1084.
[24] J.H. Davis, K.R. Jeffrey, M. Bloom, M.I. Valic, T.P. Higgs, Chem. Phys. Lett. 42 (2) (1976) 390–394.
[25] I.D. Weisman, L.H. Bennett, Phys. Rev. 181 (1969) 1341–1350.
[26] I. Solomon, Phys. Rev. 110 (1958) 61–65.
[27] S. Meiboom, D. Gill, Rev. Sci. Instrum. 29 (1958) 688–691.
[28] H.Y. Carr, Phys. Rev. 112 (1958) 1693–1701.
[29] H.Y. Carr, E.M. Purcell, Phys. Rev. 94 (1954) 630–638.
[30] T.N. Rudakov, A.V. Belyakov, J. Phys. D – Appl. Phys. 31 (10) (1998) 1251–1256.
[31] R.A. Marino, S.M. Klainer, J. Chem. Phys. 67 (7) (1977) 3388–3389.
[32] T.N. Rudakov, P.A. Hayes, J. Magn. Reson. 183 (1) (2006) 96–101.
[33] A. Gregorovic, T. Apih, J. Chem. Phys. 129 (21) (2008) 214504-1–214504-7.
[34] J.T. Cheng, P.D. Ellis, J. Phys. Chem. 93 (6) (1989) 2549–2555.
[35] F.H. Larsen, H.J. Jakobsen, P.D. Ellis, N.C. Nielsen, J. Phys. Chem. A 101 (46) (1997) 8597–8606.
[36] F.H. Larsen, H.J. Jakobsen, P.D. Ellis, N.C. Nielsen, J. Magn. Reson. 131 (1) (1998) 144–147.
[37] F.H. Larsen, J. Skibsted, H.J. Jakobsen, N.C. Nielsen, J. Am. Chem. Soc. 122 (29) (2000) 7080–7086.
[38] R. Siegel, T.T. Nakashima, R.E. Wasylishen, Concepts Magn. Reson. Part A 26A (2) (2005) 62–77.
[39] M. Rubinstein, P.C. Taylor, Phys. Rev. B 9 (10) (1974) 4258–4276.
[40] D.J. Treacy, P.C. Taylor, P.B. Klein, Solid State Commun. 32 (6) (1979) 423–427.
[41] P.C. Taylor, J. Non-Cryst. Solids 59-6 (December) (1983) 109–116.
[42] Z.M. Saleh, G.A. Williams, P.C. Taylor, Phys. Rev. B 40 (15) (1989) 10557–10563.
[43] P.C. Taylor, Z. Naturfors. Sect. A – J. Phys. Sci. 51 (5–6) (1996) 603–610.
[44] A.P. Bussandri, M.J. Zuriaga, J. Magn. Reson. 131 (2) (1998) 224–231.
[45] V. Hughes, F.R. Hartley, J. Phys. E: Sci. Instrum. 8 (12) (1975) 1027–1030.
[46] D. Hoffmann, R. Pietsch, J. Kummer, J. Phys. E: Sci. Instrum. 12 (9) (1979) 837–840.
[47] A.J. Blauch, J.L. Schiano, M.D. Ginsberg, J. Magn. Reson. 144 (2) (2000) 305–315.
[48] J.L. Schiano, A.J. Blauch, M.D. Ginsberg, Z. Naturfors. Sect. A – J Phys. Sci. 55 (1–2) (2000) 67–73.
[49] J.L. Schiano, M.D. Ginsberg, Z. Naturfors. Sect. A – J Phys. Sci. 55 (1–2) (2000) 61–66.
[50] A. Ramamoorthy, N. Chandrakumar, A.K. Dubey, P.T. Narasimhan, J. Magn. Reson. Ser. A 102 (3) (1993) 274–286.
[51] S.Z. Ageev, D.J. Isbister, B.C. Sanctuary, Mol. Phys. 83 (2) (1994) 193–210.
[52] A. Ramamoorthy, Mol. Phys. 92 (6) (1997) 1035–1038.
[53] A. Ramamoorthy, Mol. Phys. 93 (5) (1998) 757–766.
[54] C. Odin, J. Magn. Reson. 143 (2) (2000) 299–310.
[55] J.M. Bohlen, M. Rey, G. Bodenhausen, J. Magn. Res. 84 (1) (1989) 191–197.
[56] E. Van Veenendaal, B.H. Meier, A.P.M. Kentgens, Mol. Phys. 93 (2) (1998) 195–213.
[57] A.P.M. Kentgens, J. Magn. Reson. Ser. A 104 (3) (1993) 302–309.
[58] A.P.M. Kentgens, J. Magn. Reson. 95 (3) (1991) 619–625.
[59] A. Tannus, M. Garwood, NMR Biomed. 10 (8) (1997) 423–434.
[60] E. Kupce, R. Freeman, J. Magn. Reson. Ser. A 118 (2) (1996) 299–303.
[61] E. Kupce, R. Freeman, J. Magn. Reson. Ser. A 115 (2) (1995) 273–276.
[62] M. Garwood, L. DelaBarre, J. Magn. Reson. 153 (2) (2001) 155–177.
[63] R. Bhattacharyya, L. Frydman, J. Chem. Phys. 127 (19) (2007) 194503-1–194503-8.
[64] L.A. O'Dell, R.W. Schurko, Chem. Phys. Lett. 464 (1–3) (2008) 97–102.
[65] L.A. O'Dell, A.J. Rossini, R.W. Schurko, Chem. Phys. Lett. 468 (4–6) (2009) 330–335.
[66] S.Z. Ageev, B.C. Sanctuary, Chem. Phys. Lett. 225 (4–6) (1994) 499–502.
[67] C. Schurrer, S.C. Perez, Appl. Magn. Reson. 16 (1) (1999) 135–146.
[68] L.A. O'Dell, R.W. Schurko, J. Am. Chem. Soc. 131 (19) (2009) 6658–6659.
[69] S. Kroeker, R.E. Wasylishen, J.V. Hanna, J. Am. Chem. Soc. 121 (7) (1999) 1582–1590.
[70] R.K. Harris, E.D. Becker, S.M.C. De Menezes, R. Goodfellow, P. Granger, Pure Appl. Chem. 73 (11) (2001) 1795–1818.
[71] D.J. Treacy, P.C. Taylor, Solid State Commun. 40 (2) (1981) 135–138.
[72] D.J.Y. Marion, H. Desvaux, J. Magn. Reson. 193 (1) (2008) 153–157.
[73] M. Nausner, J. Schlagnitweit, V. Smrecki, X. Yang, A. Jerschow, N. Muller, J. Magn. Reson. 198 (1) (2009) 73–79.
[74] R. Lefort, J.W. Wiench, M. Pruski, J.P. Amoureux, J. Chem. Phys. 116 (6) (2002) 2493–2501.
[75] P.J. Bray, S. Moskowitz, H.O. Hooper, R.G. Barnes, S.L. Segel, J. Chem. Phys. 28 (1) (1958) 99–102.
[76] E. Fukushima, S.B.W. Roeder, Experimental Pulse NMR: A Nuts and Bolts Approach, Addison-Wesley Publishing Company, Reading, Massachusetts, 1981. p. 539.
[77] N. Veglio, M.J. Zuriaga, Appl. Magn. Reson. 28 (1–2) (2005) 107–113.
[78] Y.Y. Tong, J. Magn. Reson. Ser. A 119 (1) (1996) 22–28.
[79] D. Massiot, I. Farnan, N. Gautier, D. Trumeau, A. Trokiner, J.P. Coutures, Solid State Nucl. Magn. Reson. 4 (4) (1995) 241–248.
[80] T_2 was measured for several QCPMG sub-spectra acquired at different transmitter frequencies (Table S11) and T_2 values were found to be relatively constant, suggesting that the shape of the pattern is not strongly influenced by T_2.